GPS Solutions (2022) 26:135
https://doi.org/10.1007/s10291-022-01324-1

ORIGINAL ARTICLE

Estimating surface optical properties and thermal thrust for Galileo satellite body and solar panels

Bingbing Duan[1] · **Urs Hugentobler**[1]

Received: 5 January 2022 / Accepted: 18 August 2022 / Published online: 30 August 2022

Abstract

Precise orbit determination of GNSS (Global Navigation Satellite System) satellites requires accurate models of perturbing forces acting on the spacecraft, i.e., solar radiation pressure (SRP) and thermal radiation forces. With the officially published satellite metadata, the analytical box-wing model is usually used to describe most of the SRP accelerations and the rest is assumed to be compensated by estimating ECOM/ECOM2 (Empirical CODE Orbit Model) parameters. However, we find that the precision of Galileo satellite orbits shows notable degradation inside eclipse seasons for 3-day-arc solutions and 24-h predictions. For instance, the RMS (root-mean-square) of orbit misclosures increases by about a factor of two in the eclipse season when using the box-wing model as the a priori and the 5-parameter ECOM model on top. The reason is proven to be mostly due to ignoring imbalanced thermal radiation forces (i.e., radiator emission and thermal radiation of solar panels) as satellite thermal properties are unknown. These imbalanced thermal effects cannot be fully absorbed by the ECOM/ECOM2 parameters inside eclipse seasons because the earth's shadowing of a satellite in orbit causes periodic changes of the thermal environment. To cope with this problem, we first estimate satellite optical and thermal parameters as part of orbit determination based on Galileo tracking data covering 1 year. Then, we add physical thermal radiation models for radiators and solar panels as part of the a priori model and evaluate the performance of different ECOM models in Galileo satellite orbit determination. As shown by orbit misclosures, 24-h orbit predictions and SLR (Satellite Laser Ranging) residuals, the 7-parameter ECOM2 model performs better than the 5-parameter ECOM and the 9-parameter ECOM2 model for Galileo satellites. When using the 7-parameter ECOM2 model on top, the impact of the radiator emission and the thermal radiation of solar panels on Galileo satellite orbits is about 1 and 2 cm, respectively, inside eclipse seasons for 3-day-arc solutions.

Keywords Galileo · Thermal force modeling · Radiator emission · Solar radiation pressure · Satellite orbit determination

Introduction

Galileo is the European Global Satellite Navigation System (GNSS), providing precise positioning, navigation and timing (PNT) services. In 2005 and 2006, the first two Galileo In-Orbit Validation Element (GIOVE) satellites were launched to secure the Galileo frequencies and to flight-test some onboard satellite components (Montenbruck et al. 2006; Steigenberger et al. 2011). In 2011 and 2012, four In-Orbit Validation (IOV) satellites were launched for the assessment of the navigation payload and the infrastructure on ground. The first pair of Full Operational Capability (FOC) satellites were launched in August 2014 and the initial service capability of Galileo satellites was announced in December 2016. Currently, the operational Galileo constellation consists of 4 IOV and 22 FOC satellites. On 5 December 2021, another two Galileo satellites of the new generation were launched to reinforce Galileo satellite PNT services further.

Compared to other GNSS satellites (e.g., GPS), Galileo satellites have relatively high area-to-mass ratio, making the spacecraft more sensitive to non-gravitational forces. Also, satellite body of Galileo satellites is elongated in shape, SRP accelerations thus show a periodic pattern due to the rotation of the satellite body. Therefore, the radiation forces of Galileo satellites have to be more carefully considered in satellite orbit determination. For satellites with very

✉ Bingbing Duan
bingbing.duan@tum.de

Urs Hugentobler
urs.hugentobler@tum.de

[1] Institute for Astronomical and Physical Geodesy, Technical University of Munich, Arcisstr 21, 80333 Munich, Germany

simple spacecraft structures, Milani et al. (1987) formulate the analytical SRP model for each satellite surface based on satellite attitude law, dimensions, total mass and optical properties. For satellites with a high level of complexity in the spacecraft structure, the precise ray-tracing model is preferred if the detailed CAD model of the satellite is known (Li et al. 2018; Ziebart 2001; Ziebart and Dare 2001). In the absence of a perfect analytical model, the ECOM or hybrid ECOM model is widely used (Arnold et al. 2015; Beutler et al. 1994; Tang et al. 2021; Tseng 2021) in GNSS satellite orbit determination. Prange et al. (2017) confirm that the ECOM2 model performs much better than the 5-parameter ECOM model (Springer et al. 1999) for Galileo satellites. The reason is that higher order Fourier coefficients in the ECOM2 D direction (pointing toward the Sun) can partially absorb periodic SRP accelerations caused by the satellite body attitude motion. When combining the ECOM model with an a priori SRP model, (Montenbruck et al. 2015b; Steigenberger and Montenbruck 2017; Steigenberger et al. 2015) show that Galileo satellite orbits are clearly improved compared to the ECOM-only results.

In 2017, Galileo satellite metadata including satellite attitude law, dimensions, total mass and surface optical properties was published by the European Global Navigation Satellite Systems Agency (GSA, https://www.gsc-europa.eu/). With this metadata information, an analytical box-wing model can be formed to compensate for most of the SRP effect (Li et al. 2019). Bury et al. (2020) show that the overall accuracy of the Galileo-FOC orbits at the level of 23 mm can be obtained when considering the box-wing model as the a priori model. However, Galileo satellite orbits still show notable degradation inside eclipse seasons. This is actually the same as we have seen for other constellations, for instance for GLONASS and BeiDou satellites (Duan et al. 2020, 2021a). The reason is proven to be mostly due to ignoring the radiator emission and the thermal radiation of the solar panels as these perturbations also contribute inside the shadow, while in the shadow all the ECOM parameters are deactivated (Duan et al. 2021a). Also, thermal accelerations caused by radiators and solar panels cannot be fully absorbed by ECOM parameters.

The impact of radiator emission for Galileo satellite orbits is assessed by Sidorov et al. (2020). The emission power of radiators in the $-X$ surface is given by accumulating the power consumption of all the clocks onboard a Galileo satellite. They show that the orbit accuracy in the radial component during eclipse seasons is improved by 14% by modeling additionally the radiator thrust. Apart from the radiator thrust, Bhattarai et al. (2022) use precise ray-tracing SRP models for Galileo satellites and set up specific models to account for the SRP force caused by LRA (Laser Retroreflector Array) surfaces and thermal force for navigation antennas. The accuracy of Galileo satellite orbits is further improved to better than 2 cm in the radial component. Thermal radiation of solar panels is assessed by Vigue et al. (1994) for GPS Block II satellites based on the thermal properties of solar panels, i.e., thickness, density, heat capacity, conductivity and emissivity. The force caused by imbalanced thermal radiation of the solar panels (front and back sides) for GPS Block II satellites produces accelerations on the order of 1.0 nm/s^2 and may cause orbit errors of more than 10 m after 7 days.

In absence of officially published thermal properties of satellite surfaces, we present physical thermal radiation force models for Galileo satellites based on the estimated thermal parameters, such as radiator emission power and scaling factor of solar panel thermal thrust acceleration. We first determine satellite optical and thermal parameters using Galileo tracking data covering 1 year. Satellite attitude errors, such as solar sensor bias (causing yaw bias) and solar panel rotation lag are considered as additional parameters in the adjustment. Then, we show the impact of radiator emission and thermal radiation of solar panels on Galileo satellite orbits. Finally, we assess the performance of different ECOM models in Galileo satellite orbit determination when combining with the analytical a priori models.

Analytical radiation and thermal models

The a priori analytical radiation and thermal forces considered in this contribution consist of SRP, earth radiation (ERP), radiator emission and imbalanced thermal force of the solar panels. Milani et al. (1987) formulate the physical SRP acceleration for solar panels and satellite body surfaces (covered by Multilayer Insulation, MLI) separately. By introducing a thermal reradiation factor κ, we combine these two equations for a single surface into one equation (Duan and Hugentobler 2021)

$$\mathbf{acc}_{\mathrm{SRP}} = -\frac{A}{M}\frac{S_0}{c}\cos\theta\left[(\alpha+\delta)\mathbf{e}_D + \frac{2}{3}(\delta+\kappa\alpha)\mathbf{e}_N + 2\rho\cos\theta\mathbf{e}_N\right] \tag{1}$$

where $\mathbf{acc}_{\mathrm{SRP}}$ denotes the SRP acceleration, A the surface area, M the total mass of the satellite, S_0 the solar flux constant, c the speed of light in vacuum, κ the thermal reradiation factor (0 for solar panels and 1 for satellite body surfaces covered with MLI). α, δ, ρ represent the fractions of absorbed, diffusely scattered and specularly reflected photons. $\mathbf{e}_D$ and $\mathbf{e}_N$ denote the incident unit vector and the surface normal vector, θ the angle between both vectors. Earth radiation, a combination of albedo and infrared radiation is modeled using the same equation. The amount of earth-reflected visible solar radiation and thermal radiation is calculated from the CERES (Clouds and Earth's Radiant Energy System) (Priestley et al. 2011). A default set of

satellite infrared properties is used as given by Rodriguez-Solano et al. (2012b).

In order to dump excess heat generated by electronic devices, e.g., clocks inside the satellite body, radiators are used onboard Galileo satellites. As published by GSA, optical surface radiators are located on $-X$ and $\pm Y$ surfaces for IOV satellites and on $-X$, $\pm Y$ and $-Z$ surfaces for FOC satellites (https://www.gsc-europa.eu/). The Galileo satellite body-fixed reference frame described in this study follows the IGS (International GNSS Service) definition (Montenbruck et al. 2015a). As a Galileo satellite keeps transmitting signals continuously, we assume that heat generated by the equipment is constant over time. The radiator emission thrust can be modeled as

$$\mathbf{acc}_{\mathrm{R}} = R\mathbf{e}_N \tag{2}$$

where $\mathbf{acc}_{\mathrm{R}}$ denotes the radiator acceleration vector and R the corresponding radiator acceleration, which is unknown for Galileo satellites. We will estimate these radiator accelerations for X and Y surfaces of Galileo satellites based on tracking data covering 1 year, as described in the next section.

Radiative heat transfer between a satellite and its environment may result in imbalanced thermal forces. As shown by Cook (1989), the dominant source for imbalanced thermal force on a GPS-like satellite is the solar panels, because of their large exposed area and low heat capacity. The density of the earth's atmosphere in space at GNSS's altitude is extremely low, the only transfer mechanism between solar panels and the environment is thus thermal radiation (Walter 2018). According to Stefan Boltzmann's law the satellite solar panels emit energy at a rate that is proportional to the fourth power of the temperature and to the emissivity on both sides of the solar panels. The temperature variation of solar panels may be formulated by balancing the input energy flux from the solar radiation and the thermal reradiation on both sides of the array

$$C_{\mathrm{A}}\frac{\mathrm{d}T}{\mathrm{d}t} = \gamma(1-\eta)\alpha S_0 - \left(\varepsilon_{\mathrm{f}} + \xi\varepsilon_{\mathrm{b}}\right)\sigma T^4 \tag{3}$$

where C_{A} is the heat capacity per unit area depending on the thermal properties of solar array material, i.e., thickness, density, and specific heat (Vigue et al. 1994). γ represents the Sun illumination factor, η the electric efficiency of the solar panel, α the fractions of absorbed photons, ε_{f} and ε_{b} the emissivity on the front and back sides of the solar panels, σ the Stefan-Boltzmann constant. ξ models the temperature difference of the front and back sides of the solar panel from thermal conductivity through the panel.

The solution to this differential equation requires the specification of boundary conditions. In our computation, the boundary conditions are defined such that the temperature of the solar panels is the same after one satellite revolution. With the given temperature the imbalanced thermal acceleration can then be computed from the difference of the thermal thrust on both sides of the panel.

$$\mathrm{acc}_{\mathrm{thm}} = \frac{2}{3}\frac{A}{Mc}\left(\varepsilon_{\mathrm{f}} - \xi\varepsilon_{\mathrm{b}}\right)\sigma T^4(t) \tag{4}$$

For Galileo satellites, we assume a total thickness of the solar cells of 2 mm, an electric efficiency η of 12%, a temperature difference ξ of 0.91 (corresponding to a temperature difference of 0.02 T), and an emissivity of 0.75 on the front side and 0.90 on the back side of the solar panels. Solar cell layers and thermal properties are assumed to be similar as for GPS Block IIR satellites (Fliegel and Gallini 1996). Figure 1 shows the thermal thrust acceleration caused by thermal radiation of the solar panels. The acceleration is constant over time if the satellite is continuously illuminated, whereas it shows periodic variations when the satellite crosses the earth's shadow. As the assumptions of the thermal properties for Galileo solar panels are not accurate enough, a scaling factor S will be estimated to compensate for modeling errors, as described in the next section.

Adjustment of radiation force modeling parameters

Parameter set up

To set up precise physical radiation and thermal models, we developed a method to determine satellite optical and thermal parameters as part of orbit determination (Duan

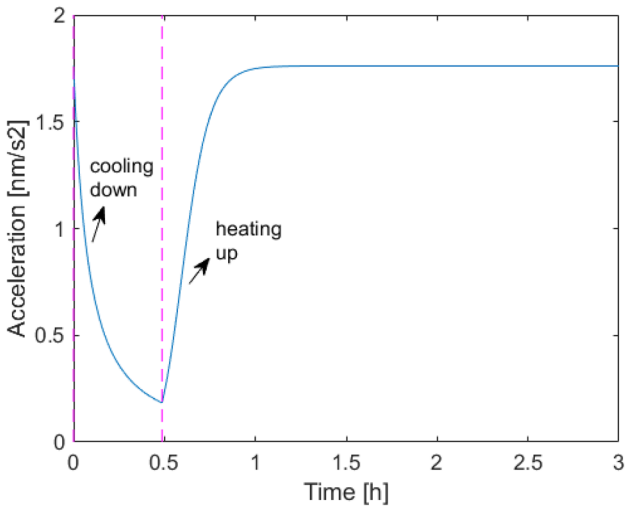

Fig. 1 Accelerations (away from the Sun) caused by imbalanced thermal force of solar panels. The dashed pink color lines indicate the shadow entering and exiting epoch

et al. 2019, 2021a). For $+X$ and $\pm Z$ surfaces (according to the IGS definition) of a Galileo satellite, two optical parameters $\alpha + \delta$ and ρ(in (1)) are estimated. The respective partial derivatives can be written as

$$\frac{\partial \mathbf{acc}_{\mathrm{SRP}}}{\partial(\alpha+\delta)} = -\frac{A}{M}\frac{S_0}{c}\cos\theta\left(\mathbf{e}_D + \frac{2}{3}\mathbf{e}_N\right) \tag{5}$$

$$\frac{\partial \mathbf{acc}_{\mathrm{SRP}}}{\partial \rho} = -\frac{A}{M}\frac{S_0}{c}\cdot 2\cos^2\theta\,\mathbf{e}_N \tag{6}$$

In the adjustment, surface normal vector ($\mathbf{e_N}$), dimension (A) and total mass (M) of the satellite are fixed to the published values. As described by Rodriguez-Solano et al. (2012a), solar panels may follow the Sun with a small lag (θ_{lag}). We estimate this lag parameter whose partial derivative can be written as

$$\frac{\partial \mathbf{acc}_{\mathrm{SRP}}}{\partial \theta_{\mathrm{lag}}} = \frac{A}{M}\frac{S_0}{c}\cdot 2\left(\frac{\delta}{3}+\rho\right)\mathrm{SIGN}(\dot{\varepsilon})\mathbf{e}_B \tag{7}$$

where $\dot{\varepsilon}$ denotes the rate of the elongation angle, the angle between the normal vector of the solar panels and the Z-axis, $\mathbf{e}_B$ represents the ECOM B direction.

GNSS satellite attitude is partly controlled by the data from solar sensors. A sensor bias may cause a yaw bias which is a function of the elongation angle

$$\sin(y\mathrm{bias}) = \sin(s\mathrm{bias})/\sin(\varepsilon) \tag{8}$$

where $s$bias denotes the sensor bias, ε the elongation angle, $y$bias the yaw bias. By rotating the satellite body by the $y$bias angle around the Z-axis, $\mathbf{e}_X$ and $\mathbf{e}_Y$ change accordingly. From the SRP differences caused by a $y$bias using (1), the numerical partial derivative can be computed to estimate the sensor bias parameter.

As radiator information in (2) for Galileo satellites is not publicly known, we estimate constant radiator accelerations in $-X$ and $+Y$ surfaces. A radiator acceleration in the $-$Z-axis is not estimated because it is fully correlated with the semi-major axis parameter in satellite orbit determination. The reason is the insensitivity of pseudorange observations on the orbit height. The constant thermal radiation force of solar panels outside eclipses is compensated by estimating the optical parameter ρ of the solar panels. The periodic thermal accelerations (cooling down and heating up parts) are corrected by estimating a scaling factor S. For the sake of simple usage, we also provide the function coefficients to direct compute the cooling down (analytical solution) and heating up (approximate solution) accelerations without the need for a deep understanding of the physical background. The analytical solution of the acceleration during cooling down is

$$\mathrm{acc}_{\mathrm{shd}} = p\left(1+\left(t-t_0\right)/\tau_c\right)^{-4/3}\cdot S \tag{9}$$

where $\mathrm{acc}_{\mathrm{shd}}$ denotes the thermal acceleration inside the shadow, p and τ_c are function coefficients, t the current time epoch and t_0 the shadow entering epoch. S represents the scaling factor that compensates for model errors caused by assumptions of solar panel thermal properties. The empirical exponential function for the acceleration during heating up is

$$\mathrm{acc}_{\mathrm{sun}} = p\left[1-e^{-\left(t_{sft}-t_h+(t-t_0)\right)/\tau_h}\right]^4\cdot S \tag{10}$$

where $\mathrm{acc}_{\mathrm{sun}}$ denotes the thermal acceleration outside the shadow, t_h and τ_h are function coefficients. t_{sft} represents a time shift assuring optimal fit to the solution of the differential equation after shadow exit

$$t_{\mathrm{sft}} = -\tau_h \log\left[1-\left(1+t_{\mathrm{shd}}/\tau_c\right)^{-1/3}\right] - t_{\mathrm{shd}} \tag{11}$$

where t_{shd} denotes the shadow duration in seconds. All the function coefficients are given in Table 1. The scaling factor S is given in Tables 3 and 4 together with other adjusted parameters. In summary, there are six optical parameters for satellite body surfaces, one optical parameters for solar panels, one solar panel rotation lag, one sensor bias, two radiator accelerations, and one scaling factor of the solar panel imbalanced thermal acceleration, i.e., in total 12 parameters for each satellite.

Parameter estimation

We estimate all the parameters using 90 globally distributed IGS MGEX (Montenbruck et al. 2017) tracking stations. The time span starts from day of year (doy) 275, 2020 to doy 274, 2021. In the first step, we compute Galileo satellite orbits using the a priori box-wing model (based on the published metadata) and the 5-parameter ECOM model on top. The geodetic datum is defined by a minimum constraint (no net rotation condition) of all the stations to the IGS14 reference frame. Earth rotation parameters are fixed to the values of the IERS Bulletin A. Earth radiation and satellite antenna thrust (Steigenberger et al. 2018) effects are modeled. Satellite antenna phase center offsets and variations (PCOs, PCVs) are corrected using the igs14.atx file. Station PCO and PCV corrections for Galileo $E1$ and $E5$a frequencies are

Table 1 Function coefficients of solar panel imbalanced thermal accelerations based on the assumed material and thermal properties

Satellite	Cooling down		Heating up	
	p (nm/s^2)	τ_c (s)	τ_h (s)	t_h (s)
IOV & FOC	1.76	393	360	50

Table 2 Processing settings

Item	Value
Software	Bernese 5.3 modified (Dach et al. 2015)
Observations	Undifferenced ionosphere-free (E1/E5a)
Ambiguity	Fixed to integer (Duan et al. 2021b)
Arc length	3-day-arc
Data sampling	5 min
Elevation cutoff	5 deg
Earth rotation parameters	Bulletin A
Earth radiation	Modeled
Antenna thrust	Modeled (IGS MGEX metadata)

assumed to be the same as those for GPS *L*1 and *L*2 frequencies. Detailed settings are given in Table 2.

In the second step, instead of estimating ECOM parameters, we estimate 12 radiation force parameters together with the 6 keplerian elements for each satellite in the orbit determination procedure. Integer ambiguities and station-related parameters that were determined in the first step are fixed as known. In a daily arc solution, the 6 orbital parameters and 12 radiation force parameters of one satellite are highly correlated, it is impossible to obtain reasonable daily solutions. To reduce high correlations between parameters, we pre-eliminate orbital parameters from daily normal equations leaving only radiation force parameters, and we stack daily normal equations over 1 year (corresponding to two times the full beta angle range) to compute reasonable radiation force parameters. Because, on the one hand, radiation force parameters do not change within 1 year (ignoring aging effects of materials), on the other hand, we have proven that correlations between parameters are greatly reduced when including full beta angle range measurements in the adjustment (Duan et al. 2019).

Tables 3 and 4 show the estimated radiation force parameters and the published optical properties of Galileo IOV and FOC satellites. Formal errors of all the estimated optical properties are smaller than 0.02. Note that the published optical properties of different materials in the same satellite body surface are combined into one set of values according to the proportion of the area of each element. The estimated optical properties show some differences of about 5–20% compared to the published values, i.e., in the $-Z$ surface of IOV satellites and in the $+X$ surface of FOC satellites. The reason could be partially due to the correlation between parameters, in particular between optical parameters and radiator parameters. However, it is also possible that optical properties change with the long-term exposure in space. Galileo IOV satellites show a radiator acceleration of -1.1 nm/s^2 in the $-X$ direction, corresponding to an emission power of about 360 W. The radiator effect in the Y surface for IOV satellites either does not exist or is balanced by both sides. The radiator acceleration for FOC satellites is -0.9 nm/s^2 and 0.68 nm/s^2 in $-X$ and $+Y$ direction, respectively, corresponding to a total emission power of about 500 W. The solar panel ρ estimates represent the constant thermal radiation of solar panels outside eclipse seasons. The scaling factor (S) estimates shows that the computed thermal acceleration in Fig. 1 is not accurate and has to be compensated by

Table 3 Galileo IOV satellite radiation force parameters, "Estimates" denotes our adjusted results, "GSA" indicates the officially published values, R represents radiator acceleration and S denotes thermal imbalance scaling factor. Satellite body-fixed frame follows the IGS definition

Surface	Area (m^2)	Estimates						GSA	
		$\alpha+\delta$	ρ	R (nm/s^2)	S	$s$bias (deg)	lag (deg)	$\alpha+\delta$	ρ
$+X$	1.320	0.950	0.017	–	–	–		1.000	0.000
$-X$	1.320	–	–	−1.10	–	–		–	–
$+Y$	3.000	–	–	−0.05	–	0.072		–	–
$+Z$	3.000	0.804	0.198	–	–	–		0.906	0.094
$-Z$	3.000	0.782	0.193	–	–	–		1.000	0.000
sp	5.410*2	0.914	0.121	–	4.878	–	0.74	0.914	0.086

Table 4 Galileo-FOC satellite radiation force parameters, "Estimates" denotes our adjusted results, "GSA" indicates the officially published values, R represents radiator acceleration and S denotes thermal imbalance scaling factor

Surface	Area (m^2)	Estimates						GSA	
		$\alpha+\delta$	ρ	R (nm/s^2)	S	$s$bias (deg)	lag (deg)	$\alpha+\delta$	ρ
$+X$	1.320	1.032	0.112	–	–	–	–	1.000	0.000
$-X$	1.320	–	–	-0.90	–	–	–	–	–
$+Y$	2.783	–	–	0.68	–	0.055	–	–	–
$+Z$	3.022	0.737	0.282	–	–	–	–	0.857	0.143
$-Z$	3.022	0.743	0.291	–	–	–	–	0.769	0.231
sp	5.410*2	0.914	0.121	–	3.396	–	0.48	0.914	0.086

Satellite body-fixed frame follows the IGS definition

the scaling factor. Galileo satellites seem to have no solar sensor bias according to our estimation but the solar panel rotation lag exists with a value smaller than 1 deg.

Galileo satellite orbit determination using different radiation force models

We use all the estimated radiation force parameters in a physical a priori model

$$\mathbf{acc}_{\mathrm{apr}} = \mathbf{acc}_{\mathrm{SRP}} + \mathbf{acc}_{y\mathrm{bias}} + \mathbf{acc}_{\mathrm{lag}} + \mathbf{acc}_{\mathrm{ERP}} + \mathbf{acc}_{R} + \mathbf{acc}_{\mathrm{sun}} + \mathbf{acc}_{\mathrm{shd}} \tag{12}$$

where $\mathbf{acc}_{\mathrm{apr}}$ denotes the total a priori acceleration, $\mathbf{acc}_{\mathrm{SRP}}$ the solar radiation pressure acceleration, $\mathbf{acc}_{y\mathrm{bias}}$ the *y*bias effect, $\mathbf{acc}_{\mathrm{lag}}$ the solar panel rotation lag effect, $\mathbf{acc}_{\mathrm{ERP}}$ the earth radiation acceleration, $\mathbf{acc}_{R}$ the radiator acceleration, $\mathbf{acc}_{\mathrm{sun}}$ and $\mathbf{acc}_{\mathrm{shd}}$ are thermal thrust accelerations of the solar panels. We use ECOM and ECOM2 models on top to assess the performance of different SRP models in Galileo satellite orbit determination. All the modeling options are given in Table 5. We use the same tracking stations and time period (1 year) as in the last section. Orbit arc length is 3 days and we extract the middle day solution as the final daily solution. Pseudo-stochastic pulses are not considered. Orbit misclosures between two consecutive arcs, 24-h orbit predictions and SLR residuals are analyzed to assess the quality of the determined Galileo satellite orbits.

We compute orbit differences at the day boundaries between consecutive arcs and define the orbit misclosure as

$$\mathbf{m}_{i,i+1} = \mathbf{r}_{s,i+1} - \mathbf{r}_{s,i} \tag{13}$$

where i and $i+1$ refer to days, $\mathbf{r}_{s,i+1}$ denotes the orbit position vector of satellite s of day $i+1$ (Lutz et al. 2016). Figure 2 illustrates the 3D (position distance) mean RMS of orbit misclosures for each modeling option. The use of the *gsa* model based on the published metadata shows reasonable improvement for all the ECOM models compared to those without any a priori model. For instance, the improvement of gsa + 7ECOM2 compared to 7ECOM2-only is about

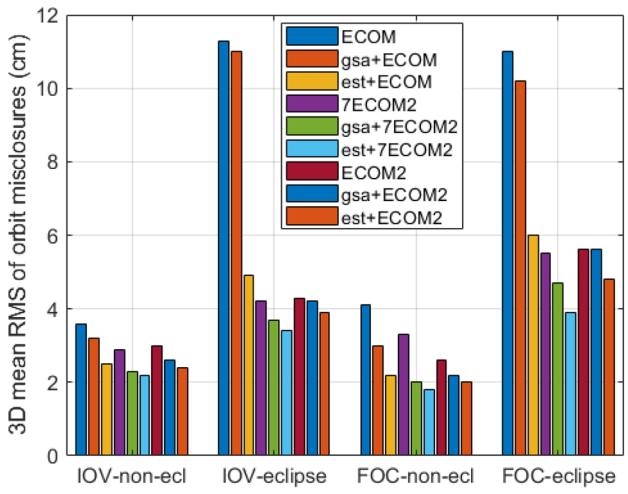

Fig. 2 3D mean RMS of orbit misclosures using different radiation force models, non-ecl denotes non-eclipsing

40% for FOC satellites outside the eclipse season. However, the ECOM-only solution inside the eclipse season is about two times worse than the ECOM2-only solution, and the use of the gsa model does not help much. When having considered thermal force models in est, the ECOM model solution inside eclipse seasons is improved by a factor of two. Thus, the imbalanced thermal forces are not negligible in satellite orbit determination, especially during eclipse seasons. The mean RMS values of all the radiation pressure models are shown in Table 6. The est + 7ECOM2 model shows the best RMS value of about 2.0 and 3.5 cm for Galileo satellites outside and inside eclipse seasons.

Satellite orbit predictions are usually used in real-time applications, the accuracy of the predicted orbits depends tightly on the radiation force models (Duan and Hugentobler 2019). As a further step to assess the performance of different radiation force models, we predict Galileo satellite orbits over 24 h based on the 3-day-arc solution. The time periods cover the same 1 year. All the predicted Galileo satellite orbits are compared to the est + 7ECOM2 daily solutions of the same epoch. Figures 3 and 4 show mean RMS values

Table 5 Items of radiation force models

Radiation pressure models	Value
ECOM	5-parameter ECOM model
gsa + ECOM	box-wing (published metadata) + ECOM
est + ECOM	physical a priori model (12) (estimated metadata) + ECOM
7ECOM2	7-parameter ECOM2 model excluding the fourth-order terms
gsa + 7ECOM2	box-wing (published metadata) + 7ECOM2
est + 7ECOM2	physical a priori model (12) (estimated metadata) + 7ECOM2
ECOM2	9-parameter ECOM2 model
gsa + ECOM2	box-wing (published metadata) + ECOM2
est + ECOM2	physical a priori model (12) (estimated metadata) + ECOM2

Table 6 3D mean RMS of orbit misclosures using different radiation pressure models (cm)

Radiation pressure models	IOV		FOC	
	Non-eclipse	Eclipse	Non-eclipse	Eclipse
ECOM	3.6	11.3	4.1	11.0
gsa + ECOM	3.2	11.0	3.0	10.2
est + ECOM	2.5	4.9	2.2	6.0
7ECOM2	2.9	4.2	3.3	5.5
gsa + 7ECOM2	2.3	3.7	2.0	4.7
est + 7ECOM2	2.2	3.4	1.8	3.9
ECOM2	3.0	4.3	2.6	5.6
gsa + ECOM2	2.6	4.2	2.2	5.6
est + ECOM2	2.4	3.9	2.0	4.8

of 24-h orbit predictions. Performances of all the modeling options are similar to those shown for the orbit misclosures. The use of the a priori gsa model based on the published metadata shows an overall improvement of about 40%, 45% and 30% over that without any a priori model for ECOM, 7ECOM2 and ECOM2 model, respectively. The use of the est model shows further improvement of about 30%, 15% and 10% compared to the use of the gsa model for ECOM, 7ECOM2 and ECOM2 model. The est + 7ECOM2 model provides the best orbit predictions. RMS values of IOV satellites are 2.0, 7.8 and 2.5 cm in radial, along-track and cross-track directions outside the eclipse season, and are 3.4, 12.2 and 4.9 cm inside the eclipse season. RMS values of FOC satellites are slightly better, with 1.1, 5.0 and 2.1 cm in radial, along-track and cross-track directions outside the eclipse season, and 3.9, 14.5 and 2.9 cm inside the eclipse season.

All the Galileo satellites are equipped with laser retroreflector arrays (LRAs). Satellite laser ranging (SLR) measurements collected by the International Laser Ranging Service (ILRS) can be used as external reference to evaluate satellite orbit results (Pearlman and Degnan 2002; Pearlman et al. 2019). Table 7 shows the mean offset and STD (standard deviation) of SLR residuals for different radiation pressure models. SLR stations that show systematic effects are excluded (Bury et al. 2021). SLR residuals exceeding ± 25 cm are not used for the statistic. SLR residuals from ECOM2 model are about two times better than those from ECOM and 7ECOM2 models without the use of any a priori model. The use of the a priori gsa or est model results in a clear improvement by combining with any ECOM model on top. For instance, the STD value is reduced by about 60% for the ECOM and 7ECOM2 model, and by about 25% for the ECOM2 model. However, the use of the *gsa* model increases the mean residual value from less than 1 cm to about 3 cm for FOC satellites, whereas, it decreases to almost zero when using the est model. In general, est + 7ECOM2 model shows the best SLR residuals.

Impact of individual radiation forces on satellite orbits

In order to show the impact of each term in (12) on Galileo satellite orbits, we take the est + 7ECOM2 solution as the reference and evaluate satellite orbits that are determined by ignoring one of the radiation forces in (12). All the settings are the same as in the previous sections. The ERP effect is confirmed by Rodriguez-Solano et al. (2012b) to have an impact of about 1–2 cm in the radial direction, and therefore,

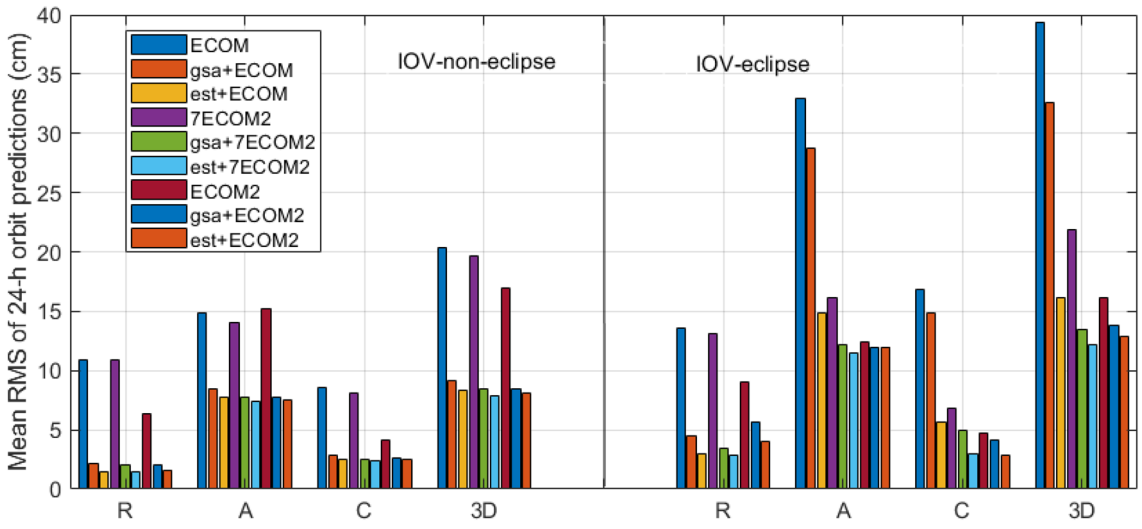

Fig. 3 RMS values of 24-h orbit predictions from comparing each radiation force model results to the est + 7ECOM2 daily results. *R* denotes radial, *A* along-track, *C* cross-track and 3D the 3D position distance (IOV satellites)

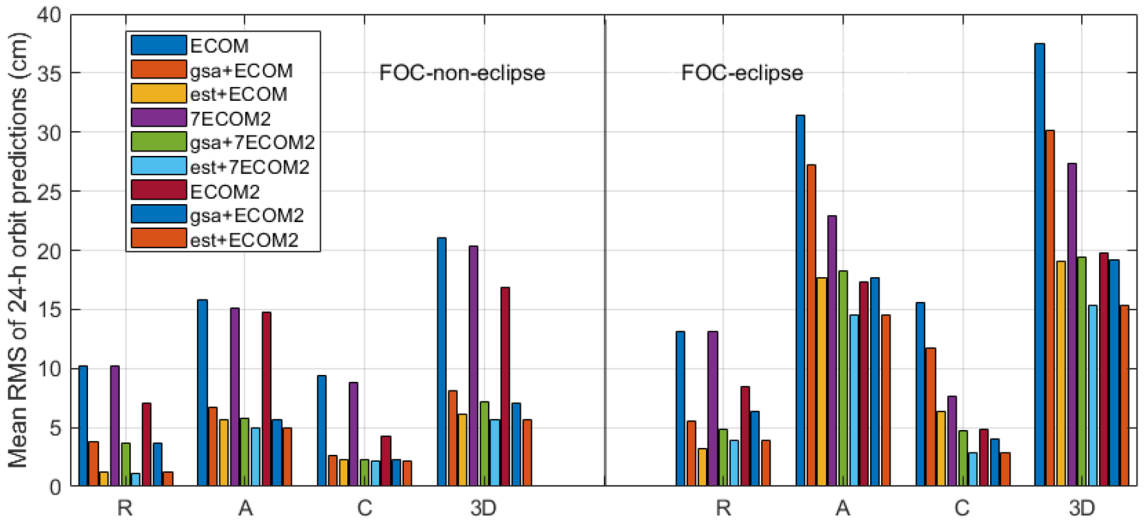

Fig. 4 RMS values of 24-h orbit predictions from comparing each radiation force model results to the est + 7ECOM2 daily results. *R* denotes radial, *A* along-track, *C* cross-track and 3D the 3D position distance (FOC satellites)

Table 7 Mean offset and STD values of SLR residuals (cm)

Radiation models	IOV		FOC	
	Mean	STD	Mean	STD
ECOM	−2.2	9.0	−1.0	8.5
gsa + ECOM	−0.4	3.7	3.3	3.5
est + ECOM	0.4	3.5	−0.1	3.4
7ECOM2	−2.0	9.0	−0.8	8.5
gsa + 7ECOM2	−0.5	3.5	3.3	3.5
est + 7ECOM2	0.4	3.5	−0.1	3.4
ECOM2	0.1	5.2	0.2	5.0
gsa + ECOM2	−0.5	4.3	3.1	3.8
est + ECOM2	0.2	3.8	−0.2	3.5

In total 31,480 SLR measurements are used

we do not repeat the analysis. The yaw bias angle for Galileo satellites is very close to zero and does not need to be considered. The importance of the a priori SRP model for Galileo satellites is clear, we can already draw conclusions from our aforementioned results. The interesting point is whether our estimated Galileo satellite optical properties perform better than the published values in Galileo satellite orbit determination. So, in this section we first assess both sets of optical parameters in satellite orbit determination, considering no other physical effects but only the a priori SRP box-wing model.

Table 8 shows RMS values of orbit misclosures and statistics of SLR residuals using the published (GSA) and the estimated surface optical parameters. The a priori box-wing model and the 7ECOM2 model are used, thermal radiation forces and other physical effects are not considered. As seen from orbit misclosures. a minor improvement (1 mm) is observed when using the estimated optical values. The STD values of SLR residuals are almost the same when using both parameters, but an improvement of the mean offset for FOC satellites is clearly visible when using our estimated optical parameters. Therefore, the estimated optical parameters of Galileo satellites are preferred.

Then, we show the impact of solar panel rotation lag, radiator emission and thermal radiation of the solar panels on Galileo satellite orbits. Figure 5 shows the daily RMS of orbit differences by ignoring solar panel rotation lag, radiator emission and thermal radiation of solar panels separately (Galileo E03 satellite is taken as an example). All the solutions employ the 7ECOM2 model on top and are compared

Table 8 RMS of orbit misclosures and statistics of SLR residuals (cm) using the published optical parameters (GSA) and our estimated optical parameters (Estimate), thermal forces and other physical effects are not considered

Optical parameters	Orbit misclosure				SLR			
	IOV		FOC		IOV		FOC	
	Non-eclipse	Eclipse	Non-eclipse	Eclipse	Mean	STD	Mean	STD
GSA	2.3	3.7	2.0	4.7	−0.5	3.5	3.3	3.5
Estimate	2.2	3.7	1.9	4.7	0.3	3.4	−0.2	3.4

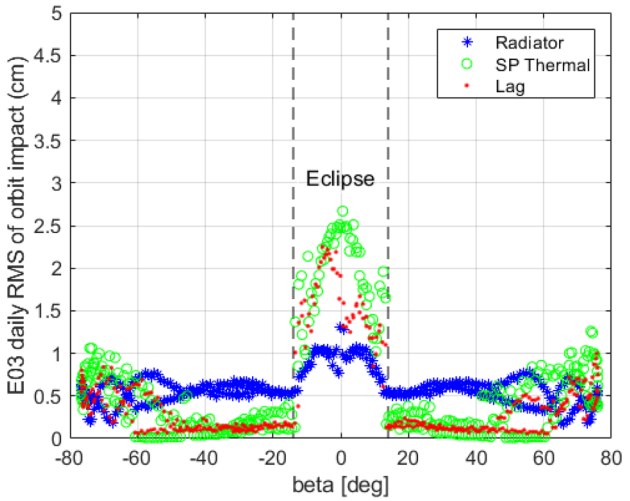

Fig. 5 Impact of solar panel rotation lag, radiator emission and thermal radiation of solar panels on Galileo (E03) satellite orbits as a function of β angle. SP Thermal denotes thermal radiation of solar panels

to the reference solution (est + 7ECOM2). Solar panel rotation lag and thermal radiation of solar panels are correlated and have a notable impact of 1–3 cm in the eclipse season. In the non-eclipse season, the impact of these two perturbations is close to zero because the lag and thermal effects of solar panels in this case can be well absorbed by the ECOM BS (sine term in the B direction) and D0 (constant term in the D direction) parameter, respectively. We can also find that when the absolute value of the β angle (Sun elevation above the orbital plane) is larger than 60 deg the mean impact of solar panel rotation lag and thermal radiation of solar panels is about 0.5 cm. This is because one of the other two orbital planes during this time period is in the eclipse season, satellite orbit solutions of the *E*03 orbital plane are affected through other common parameters, i.e., receiver clock offsets and station coordinates. The radiator thrust shows an overall impact of about 0.5 and 1.0 cm on satellite orbits outside and inside the eclipse season. The mean RMS of all satellites for all these three perturbations are given in Table 9.

Summary and outlook

This contribution aims to set up precise thermal radiation force models for Galileo satellites. In the absence of published thermal properties, we estimate thermal modeling parameters together with optical parameters and attitude bias parameters as part of orbit determination. The current result shows that the estimated surface optical properties of Galileo satellites have differences of about 5–20% in different satellite surfaces ($+X$ and $\pm Z$) compared to the published values.

Table 9 Mean RMS of orbit differences by ignoring solar panel rotation lag, radiator emission or thermal radiation of solar panels (cm)

Forces	IOV		FOC	
	Non-eclipse	Eclipse	Non-eclipse	Eclipse
Lag	0.2	0.5	0.2	1.3
Radiator	0.5	1.0	0.5	0.8
SP thermal	0.3	2.7	0.3	1.9

These differences cause 1 mm differences in the RMS of orbit misclosures and in the STD of SLR residuals, but cause about 3 cm differences in the mean offset of SLR residuals for the FOC satellites. All the Galileo satellites have no yaw bias according to our estimation, but have a rotation lag of about 0.7 and 0.5 deg for IOV and FOC satellite, respectively. Without any yaw bias, the *Y*-bias estimates of the FOC satellites are dominated by the radiator thrust in the *Y* surface. The emission power of radiators on the $-X$ surface for IOV satellites is about 360 W, while the total emission power of radiators on the $-X$ and *Y* surfaces for FOC satellites is about 500 W. Thermal radiation of solar panels is first calibrated by using a physical thermal radiation model based on some assumed material compositions and thermal properties. Then, thermal radiation modeling errors are compensated by estimating a scaling factor using tracking data covering 1 year.

With the box-wing SRP model and all the thermal radiation models, it is evident that Galileo satellite orbits are further improved compared to solutions using only the box-wing model and ECOM models (ECOM, 7ECOM2 and ECOM2). In particular, the improvement for the 5-parameter ECOM model is more than a factor of two in the eclipse season. The est + 7ECOM2 model shows the best orbit misclosure of about 2.0 and 3.5 cm outside and inside eclipse seasons. When predicting orbit solutions over 24 h the use of the a priori est model shows an improvement of about 30%, 15% and 10% over the gsa model for ECOM, 7ECOM2 and ECOM2 model, respectively. However, we observe minor improvement in SLR residuals (STD value) by considering thermal radiation effects since imbalanced thermal perturbations affect satellite orbits mainly in the along- and cross-track directions.

To assess the impact of solar panel rotation lag, radiator effects and thermal radiation of solar panels, we use the 7ECOM2 model on top and ignore each of these perturbations one by one. Radiator effects of Galileo satellites have an impact of about 0.5 cm and 1.0 cm on satellite orbits outside and inside eclipse seasons. Solar panel rotation lag and thermal radiation of solar panels have minor impact on satellite orbit outside eclipses, because the lag and thermal effects of solar panels can be very well absorbed by the ECOM BS and D0 parameter, respectively. Although we

compute the impact of lag and thermal effects of solar panels inside the eclipse season individually, correlations between these two effects cannot be avoided. It makes more sense to summarize the total impact of both perturbations, which is 3.2 cm for both types of Galileo satellites inside the eclipse season if the 7ECOM2 is used on top.

Acknowledgments This research is based on the analysis of Galileo measurements provided by the IGS MGEX (publicly available). SLR measurements are provided by ILRS. The effort of all the agencies and organizations as well as all the data centers and analysis centers is acknowledged. Calculations are based on the Bernese GNSS Software (license available, University of Bern) and its specific modifications by the authors (not public).

Funding Open Access funding enabled and organized by Projekt DEAL.

Data availability Galileo satellite RINEX and SLR observations are downloaded from (ftp://gdc.cddis.eosdis.nasa.gov). The Galileo satellite metadata is made available by the European Global Navigation Satellite Systems Agency (GSA, https://www.gsc-europa.eu/).

References

Arnold D, Meindl M, Beutler G, Dach R, Schaer S, Lutz S, Prange L, Sośnica K, Mervart L, Jäggi A (2015) CODE's new solar radiation pressure model for GNSS orbit determination. J Geodesy 89(8):775–791

Beutler G, Brockmann E, Gurtner W, Hugentobler U, Mervart L, Rothacher M, Verdun A (1994) Extended orbit modeling techniques at the CODE processing center of the international GPS service for geodynamics (IGS): theory and initial results. Manuscr Geodaet 19(6):367–386

Bhattarai S, Ziebart M, Springer T, Gonzalez F, Tobias G (2022) High-precision physics-based radiation force models for the Galileo spacecraft. Adv Space Res 69(12):4141–4154. https://doi.org/10.1016/j.asr.2022.04.003

Bury G, Sośnica K, Zajdel R, Strugarek D (2020) Toward the 1-cm Galileo orbits: challenges in modeling of perturbing forces. J Geod 94(2):1–19

Bury G, Sośnica K, Zajdel R, Strugarek D, Hugentobler U (2021) Determination of precise Galileo orbits using combined GNSS and SLR observations. GPS Solut 25(1):1–13

Cook RA (1989) The effects of thermal imbalance forces on simple spacecraft. University of Texas at Austin

Dach R, Lutz S, Walser P, Fridez P (2015) Bernese GNSS software version 5.2, User manual. Astronomical institute, University of Bern, Switzerland, Bern Open Publishing https://doi.org/10.7892/boris.72297

Duan B, Hugentobler U (2021) Enhanced solar radiation pressure model for GPS satellites considering various physical effects. GPS Solut. https://doi.org/10.1007/s10291-020-01073-z

Duan B, Hugentobler U, Selmke I (2019) The adjusted optical properties for Galileo/BeiDou-2/QZS-1 satellites and initial results on BeiDou-3e and QZS-2 satellites. Adv Space Res 63(5):1803–1812

Duan B, Hugentobler U, Hofacker M, Selmke I (2020) Improving solar radiation pressure modeling for GLONASS satellites. J Geod. https://doi.org/10.1007/s00190-020-01400-9

Duan B, Hugentobler U, Selmke I, Marz S, Killian M, Rott M (2021a) BeiDou satellite radiation force models for precise orbit determination and geodetic applications. IEEE Trans Aerosp Electron Syst. https://doi.org/10.1109/TAES.2021.3140018

Duan B, Hugentobler U, Selmke I, Wang N (2021) Estimating ambiguity fixed satellite orbit, integer clock and daily bias products for GPS L1/L2, L1/L5 and Galileo E1/E5a, E1/E5b signals. J Geod. https://doi.org/10.1007/s00190-021-01500-0

Duan B, Hugentobler U (2019) GNSS orbit prediction with enhanced solar radiation pressure model. In: China satellite navigation conference, Springer, pp 16–23

Fliegel HF, Gallini TE (1996) Solar force modeling of block IIR global positioning system satellites. J Spacecr Rocket 33(6):863–866

Li Z, Ziebart M, Bhattarai S, Harrison D, Grey S (2018) Fast solar radiation pressure modelling with ray tracing and multiple reflections. Adv Space Res 61(9):2352–2365

Li X, Yuan Y, Huang J, Zhu Y, Wu J, Xiong Y, Li X, Zhang K (2019) Galileo and QZSS precise orbit and clock determination using new satellite metadata. J Geod 93(8):1123–1136

Lutz S, Meindl M, Steigenberger P, Beutler G, Sośnica K, Schaer S, Dach R, Arnold D, Thaller D, Jäggi A (2016) Impact of the arc length on GNSS analysis results. J Geod 90(4):365–378

Milani A, Nobili AM, Farinella P (1987) Non-gravitational perturbations and satellite geodesy. Adam Hilger, Bristol

Montenbruck O, Günther C, Graf S, Garcia-Fernandez M, Furthner J, Kuhlen H (2006) GIOVE-A initial signal analysis. GPS Solut 10(2):146–153

Montenbruck O, Schmid R, Mercier F, Steigenberger P, Noll C, Fatkulin R, Kogure S, Ganeshan AS (2015a) GNSS satellite geometry and attitude models. Adv Space Res 56(6):1015–1029

Montenbruck O, Steigenberger P, Hugentobler U (2015b) Enhanced solar radiation pressure modeling for Galileo satellites. J Geod 89(3):283–297

Montenbruck O, Steigenberger P, Prange L, Deng Z, Zhao Q, Perosanz F, Romero I, Noll C, Stürze A, Weber G (2017) The Multi-GNSS experiment (MGEX) of the international GNSS service (IGS)–achievements, prospects and challenges. Adv Space Res 59(7):1671–1697

Pearlman M, Degnan JJ (2002) The International laser ranging service. Adv Space Res 30(2):135–141

Pearlman MR, Noll CE, Pavlis EC, Lemoine FG, Combrink L, Degnan JJ, Kirchner G, Schreiber U (2019) The ILRS: approaching 20 years and planning for the future. J Geod 93(11):2161–2180

Prange L, Orliac E, Dach R, Arnold D, Beutler G, Schaer S, Jäggi A (2017) CODE's five-system orbit and clock solution: the challenges of multi-GNSS data analysis. J Geod 91(4):345–360

Priestley KJ, Smith GL, Thomas S, Cooper D, Lee Iii RB, Walikainen D, Hess P, Szewczyk ZP, Wilson R (2011) Radiometric performance of the CERES Earth radiation budget climate record sensors on the EOS Aqua and Terra spacecraft through April 2007. J Atmos Oceanic Tech 28(1):3–21

Rodriguez-Solano C, Hugentobler U, Steigenberger P (2012a) Adjustable box-wing model for solar radiation pressure impacting GPS satellites. Adv Space Res 49(7):1113–1128

Rodriguez-Solano C, Hugentobler U, Steigenberger P, Lutz S (2012b) Impact of earth radiation pressure on GPS position estimates. J Geod 86(5):309–317
Sidorov D, Dach R, Polle B, Prange L, Jäggi A (2020) Adopting the empirical CODE orbit model to Galileo satellites. Adv Space Res 66(12):2799–2811
Springer TA, Beutler G, Rothacher M (1999) Improving the orbit estimates of GPS satellites. J Geod 73(3):147–157
Steigenberger P, Montenbruck O (2017) Galileo status: orbits, clocks, and positioning. GPS Solut 21(2):319–331
Steigenberger P, Hugentobler U, Montenbruck O, Hauschild A (2011) Precise orbit determination of GIOVE-B based on the CONGO network. J Geod 85(6):357–365
Steigenberger P, Montenbruck O, Hugentobler U (2015) GIOVE-B solar radiation pressure modeling for precise orbit determination. Adv Space Res 55(5):1422–1431
Steigenberger P, Thoelert S, Montenbruck O (2018) GNSS satellite transmit power and its impact on orbit determination. J Geod 92(6):609–624
Tang L, Wang J, Zhu H, Ge M, Xu A, Schuh H (2021) A comparative study on the solar radiation pressure modeling in GPS precise orbit determination. Remote Sens 13(17):3388
Tseng T-P (2021) A hybrid ECOM model for solar Radiation pressure effect on GPS reference orbit derived by orbit fitting technique. Remote Sens 13(22):4681
Vigue Y, Schutz BE, Abusali P (1994) Thermal force modeling for global positioning system using the finite element method. J Spacecr Rocket 31(5):855–859
Walter U (2018) Astronautics the physics of space flight. Wiley, New York
Ziebart M, Dare P (2001) Analytical solar radiation pressure modelling for GLONASS using a pixel array. J Geod 75(11):587–599
Ziebart M (2001) High precision analytical solar radiation pressure modelling for GNSS spacecraft. University of East London

Bingbing Duan is working at the Institute for Astronomical and Physical Geodesy, TUM, Germany. His main research interests are GNSS orbit modeling, precise GNSS orbit determination, GNSS signal biases, PPP-AR, LEO satellite orbit determination, and the combination of space techniques (GNSS, DORIS, SLR).

Urs Hugentobler is a professor at TUM, Germany, and head of the Research Facility Satellite Geodesy. His research activities focus on precise GNSS applications such as positioning, precise orbit determination, reference frame realization, time transfer, and other space techniques, such as DORIS, SLR, and VLBI.